Osteoporosis International (2019) 30:1089–1098
https://doi.org/10.1007/s00198-019-04884-0

ORIGINAL ARTICLE

Differentially expressed proteins identified by TMT proteomics analysis in bone marrow microenvironment of osteoporotic patients

Q. Zhou[1] · F. Xie[1] · B. Zhou[2] · J. Wang[1] · B. Wu[1] · L. Li[1] · Y. Kang[2] · R. Dai[1] · Y. Jiang[3]

Received: 31 August 2018 / Accepted: 28 January 2019 / Published online: 9 February 2019

Abstract

Summary We applied tandem mass tag (TMT)-based proteomics to investigate protein changes in bone marrow microenvironment of osteoporotic patients undergoing spine fusion. Multiple bioinformatics tools were used to identify and analyze 219 differentially expressed proteins. These proteins may be associated with the pathogenesis of osteoporosis.

Introduction Bone marrow microenvironment is indispensable for the maintenance of bone homeostasis. We speculated that alterations of some factors in the microenvironment of osteoporotic subjects might influence the homeostasis. This study aimed to investigate the changes in the expression of protein factors in the bone marrow environment of osteoporosis.

Methods We performed a proteomics analysis in the vertebral body-derived bone marrow supernatant fluid from 8 Chinese patients undergoing posterior lumbar interbody fusion (4 osteoporotic vs. 4 non-osteoporotic) and used micro-CT to analyze the microstructural features of spinous processes from these patients. We further performed western blotting to validate the differential expressions of some proteins.

Results There was deteriorated bone microstructure in osteoporotic patients. Based on proteomics analysis, 172 upregulated and 47 downregulated proteins were identified. These proteins had multiple biological functions associated with osteoblast differentiation, lipid metabolism, and cell migration, and formed a complex protein–protein interaction network. We identified five major regulatory mechanisms, splicing, translation, protein degradation, cytoskeletal organization, and lipid metabolism, involved in the pathogenesis of osteoporosis.

Conclusions There are various protein factors, such as DDX5, PSMC2, CSNK1A1, PLIN1, ILK, and TPM4, differentially expressed in the bone marrow microenvironment of osteoporotic patients, providing new ideas for finding therapeutic targets for osteoporosis.

Keywords Bone marrow microenvironment · Bone marrow supernatant fluid · Bone microstructure · Osteoporosis · Proteomics

Introduction

Osteoporosis is a systemic bone disease characterized by compromised bone mass and bone quality with an increased risk of fractures [1]. Bone is a dynamic system made up of several cell types including BMSCs, osteoblasts, osteoclasts, vascular endothelial cells, and their microenvironment [2]. Cells in the bone marrow locally produce soluble factors for intercellular communication, forming the bone marrow microenvironment [3]. The bone marrow microenvironment is the paramount site for bone remodeling, which is precisely modulated by osteoblastic bone formation and osteoclastic bone resorption [4]. Imbalance of bone formation and resorption may generate several bone disorders, including osteoporosis. Besides, osteoblasts and adipocytes in the bone marrow share the common precursors, bone marrow mesenchymal stem cells (BMSCs). Any disturbance in the bone marrow microenvironment may influence BMSCs' fate, contributing to the destruction of bone homeostasis [3, 5]. For example, increased reactive oxygen species in bone marrow inhibits osteoblastic differentiation

✉ R. Dai
dairuchun@csu.edu.cn

[1] Department of Metabolism and Endocrinology, Hunan Provincial Key Laboratory for Metabolic Bone Diseases, National Clinical Research Center for Metabolic Diseases, the Second Xiangya Hospital, Central South University, Changsha 410011, Hunan, China

[2] Department of Spine Surgery, the Second Xiangya Hospital, Central South University, Changsha 410011, Hunan, China

[3] Osteoporosis and Arthritis Lab, University of Michigan, Ann Arbor, MI 48109, USA

of BMSCs [6]. Also, bone marrow adipocytes release adipokines to influence the marrow microenvironment and inhibits differentiation of osteoblasts [7, 8]. Our previous work found that microarchitectures of autografts deteriorated severely in osteoporotic patients undergoing spine fusion [9]. However, it is still unknown what changes of factors in the bone marrow microenvironment have occurred under pathological condition.

As the anatomical region of bone is complicated, research on bone marrow microenvironment is difficult to perform. Some previous proteomics studies on osteoporosis have identified certain molecules inferred from protein profiling of peripheral blood [10–14], but to date, there is no study on bone marrow using proteomics technology in the field of osteoporosis research. Compared to peripheral blood, measurements of molecules in bone marrow supernatant fluid (BMSF) can directly and veritably reflect the local physiological and pathological states of the bone marrow microenvironment [15–17], thus providing a way to study bone marrow changes and underlying molecular mechanisms of osteoporosis.

Mass spectrometry (MS)-based proteomics analysis is an optimal technology to investigate relative amounts and changes of proteins. MS/MS-based proteomics strategies using tandem mass tags (TMT) have become a powerful and popular strategy in recent years [18]. By using isotopomer labels, proteins in different specimens can be simultaneously identified and quantified with high precision [19].

Since the bone marrow microenvironment is indispensable for the maintenance of bone homeostasis, we hypothesize that certain factors in the microenvironment of osteoporotic subjects may influence the homeostasis. To investigate the changes of protein factors in the bone marrow microenvironment of osteoporotic bone, we applied the TMT-based proteomics technique to integrally analyze differentially expressed proteins in BMSF between osteoporosis (OP) and non-osteoporosis (non-OP). It may provide new ideas for further research on the mechanism of osteoporosis and the discovery of therapeutic targets.

Methods

Study subjects and sample processing

All participants were recruited from the Department of Spine Surgery, the Second Xiangya Hospital, Central South University, China. We recruited patients who were diagnosed with single-segment lumbar degenerative, spondylolisthesis or spinal stenosis by radiographic examination, and needed to be treated with posterior lumbar interbody fusion (PLIF), which was performed by the same surgery team led by Yijun Kang. Dual-energy X-ray absorptiometry (Hologic Delphi A; Hologic, Bedford, MA, USA) was applied to perform bone mineral density (BMD) examination on each patient 2–3 days before undergoing PLIF. Exclusion criteria included infection, tumor, acute vertebral fractures, spinal tuberculosis, ankylosing spondylitis, severe spinal deformities, osteomalacia, coagulopathy, renal insufficiency, lumbar surgery history, anti-osteoporosis treatment history, and diseases that affect bone metabolism, such as thyroid disease, parathyroid disease, adrenal disease, and diabetes. There was no use of bone induction products during PLIF. We randomly selected 8 patients (6 Chinese postmenopausal females and 2 Chinese age ≥ 50 males) for TMT-based proteomics studies, including OP ($T \leq -2.5$ at the femoral neck or lumbar spine 1–4) and non-OP ($T > -2.5$ at both sites). The group of these 8 patients was defined as the discovery group. Bone marrow was obtained from the vertebral body at L4/5 during PLIF and centrifuged at 600×g for 5 min at 4 °C to obtain BMSF [16]. The BMSF specimens were stored at − 80 °C for follow-up experiments. To test the accuracy and repeatability of TMT-based high-throughput strategy, we performed western blotting to verify some differentially expressed proteins in these 8 patients (discovery group) and another 8 newly enrolled patients (6 Chinese postmenopausal females and 2 Chinese age ≥ 50 males), including OP and non-OP, who were randomly selected according to the same diagnostic criteria and exclusion criteria. The group of all these 16 patients was defined as the validation group. This study obtained the ethics approval from the ethical committee of the Second Xiangya Hospital. The demographic data of the study subjects are shown in Table 1.

Micro-CT

Spinous processes of patients in the discovery group were scanned by micro-CT as previously described [9]. Briefly, the autologous spinous process was obtained at L4/5 during PLIF and made into a cancellous bone cube (5 mm × 5 mm × 5 mm) by diamond blade. Microstructural features of cancellous bone cubes were scanned and analyzed by micro-CT (SkyScan1176, Bruker microCT, Kontich, Belgium).

Sample preparation for TMT-based proteomics analysis

BMSF samples were taken from − 80 °C and IgG/Albumin high-abundance proteins were removed. After 12,000×g, 10 min, 4 °C centrifugation, the protein concentrations of supernatant samples were measured. Dithiothreitol (Sigma) was added to these samples at 5 mM and incubated at 56 °C for 30 min. Iodoacetamide (Sigma) was then added at 11 mM and incubated at room temperature for 15 min in the dark. TEAB (Sigma) was added to dilute samples. Samples were then digested by trypsin (Promega) at 50:1 (protein trypsin) mass ratio overnight and 100:1 for 4 h. Subsequently, peptides were desalted by Strata X C18 (Phenomenex) and vacuum-

Table 1 Patient characteristics of the discovery and validation group

	Discovery group		*p* value	Validation group		*p* value
	non-OP ($n = 4$)	OP ($n = 4$)		non-OP ($n = 8$)	OP ($n = 8$)	
Female/male	3/1	3/1		6/2	6/2	
Age (year)	54.0 ± 1.1	56.3 ± 2.3	0.414	56.1 ± 1.5	57.1 ± 1.4	0.631
BMI (kg/m^2)	23.62 ± 1.05	21.40 ± 1.40	0.251	24.79 ± 0.89	22.11 ± 0.83	0.045*
BMD-S (g/cm^2)	1.02 ± 0.06	0.71 ± 0.04	0.005*	0.99 ± 0.03	0.73 ± 0.02	0.000*
BMD-Hip (g/cm^2)	0.91 ± 0.02	0.67 ± 0.11	0.089	0.90 ± 0.02	0.71 ± 0.06	0.008*
Time (year)	4.0 ± 1.0$^{\#}$	7.7 ± 1.8$^{\#}$	0.145	5.0 ± 1.4$^{\&}$	8.0 ± 1.5$^{\&}$	0.186

*$p < 0.05$, $^{\#}n = 3$, $^{\&}n = 6$; BMD-S, total BMD at lumbar spine (L1-L4); BMD-Hip, total BMD at hip; Time, menopause duration

dried. The peptides were dissolved in 0.5 M TEAB and labeled based on the TMT kit (Thermo) instructions. TMT reagent was dissolved in acetonitrile (Fisher Chemical) and added to peptides incubating for 2 h. Each individual subject was labeled with a unique reporter. Then the mixtures were pooled, desalted, and vacuum-dried.

High-performance liquid chromatography (HPLC) fractionation

Agilent 300Extend C18 column (5 μm particle size, 4.6 mm ID, 250 mm length) was used to fractionate peptides. Briefly, the parameters were set as 8–32% acetonitrile (pH 9.0). Peptides were fractionated into 60 fractions in 60 min, and combined into 18 fractions. The combined fractions were then subjected to vacuum-dried.

LC-MS/MS analysis

The peptides were dissolved in solvent A (0.1% formic acid) and separated using EASY-nLC 1000 UPLC (Thermo). The parameters were set as 7–25% solvent B (0.1% formic acid and 90% acetonitrile) for 24 min, 25–40% for 8 min, 40–80% for 4 min, and 80% for 4 min at 350 nL/min flow rate. Peptides were then subjected to the NSI ion source and analyzed by Q Exactive Plus (Thermo). The MS scan was set as 350–1800 m/z and 70,000 resolution; the MS/MS scan was set as 100 m/z and 17,500 resolution. The data-dependent acquisition procedure was applied to data acquisition. Automatic gain control was set as 5E4. The dynamic exclusion time was 30 s. The MS/MS data were then analyzed using MaxQuant (v.1.5.2.8). Searches were made against SwissProt Human database (20,130 proteins) and reverse decoy database. The missing cleavage was set to 2. For precursor ions, the mass tolerances of first search and main search were 20 ppm and 5 ppm, respectively. The mass tolerance of fragment ions was 0.02 Da. FDR was adjusted to < 1%.

Bioinformatics analysis

Differentially expressed proteins were identified using 1.3-fold change and the Wilcoxon-test $p < 0.05$ threshold. Subsequently, multiple bioinformatics tools were performed to analyze these proteins. UniProt-GOA was used to generate Gene Ontology (GO) annotation. The Kyoto Encyclopedia of Genes and Genomes (KEGG) database was used to analyze enriched pathways. For GO and KEGG enrichment analyses, two-tailed Fisher's exact test was applied to test differentially expressed proteins against all identified proteins. Corrected $p < 0.05$ was considered significant. STRING database (v.10.5) was used for constructing protein–protein interaction (PPI) network. The minimum interaction score was 0.400 and the *k*-means clustering was applied. Further, Cytoscape (v.3.6.0) software was applied to visualize the network.

Western blotting validation

BMSF samples were lysed with RIPA (Beyotime Biotechnology), and centrifugated at 12,000 rpm for 10 min at 4 °C. Samples were separated by 10% SDS-PAGE and then transferred onto nitrocellulose membranes. Anti-DDX5 (10804-1-AP, Proteintech), PSMC2 (14905-1-AP, Proteintech), CSNK1A1 (55192-1-AP, Proteintech), PLIN1 (ab172907, Abcam), ILK (12955-1-AP, Proteintech), TPM4 (13741-1-AP, Proteintech), and GAPDH (10494-1-AP, Proteintech) antibodies were used to incubate membranes. Bands were detected by chemiluminescence and analyzed by Quantity One (Bio-Rad).

Statistical analysis

Data were presented as mean ± SEM. Data distributions were assessed by the Kolmogorov–Smirnov test. Student's *t* test was applied to analyze patient characteristics, bone microstructural features and western blotting results of OP and non-OP. $P < 0.05$ was considered significant.

Results

Clinical characteristics of patients

There were 12 postmenopausal females and 4 aged males (≥ 50 years old) who were recruited, of which 6 females and 2 males were enrolled in the discovery group. Age, gender, body mass index (BMI), and menopause duration showed no significant difference between OP and non-OP in the discovery group ($p > 0.05$). Also, there was no significant difference between the OP and non-OP in the validation group in terms of age, gender and menopause duration ($p > 0.05$). Total BMD at the lumbar spine (L1-L4) was significantly decreased in the OP of discovery group and validation group ($p < 0.05$). Total BMD at the hip was significantly decreased in the OP of the validation group ($p < 0.05$) (Table 1).

Bone microstructural features of the discovery group

We applied micro-CT to test the microstructural features of the spinous process from the discovery group. OP had significantly lower bone volume density (BV/TV), bone surface density (BS/TV) and trabecular number (Tb.N), and higher structure model index (SMI) which suggested trabecula inclined to be a more rod-like structure. Specific bone surface (BS/BV), trabecular thickness (Tb.Th), trabecular separation (Tb.Sp), and connectivity density (Conn.D.) showed no significant difference between non-OP and OP (Table 2). The micro-CT scanning results showed that bone mass was decreased and trabecular architecture was impaired in OP. These revealed that the bone microstructure was deteriorated in OP compared with non-OP.

Identification of differentially expressed proteins in BMSF

TMT-based proteomics was performed to screen the differentially expressed proteins in BMSF between non-OP and OP of the discovery group. In total, 10,915 unique peptides were detected based on the MS/MS spectrum database search analysis, corresponding to 2002 proteins, of which 1718 proteins were identified with quantitative information in each single subject. For further analysis, we used the 1.3-fold change standard and Wilcoxon-test $p < 0.05$ threshold. Among these 1718 proteins, 172 proteins were upregulated and 47 were downregulated in OP.

Table 2 Bone microstructural features of the discovery group

	non-OP ($n = 4$)	OP ($n = 4$)	p value
BV/TV (%)	20.54 ± 1.79	11.03 ± 0.48	0.002*
BS/BV (mm^{-1})	20.67 ± 3.07	24.90 ± 1.63	0.283
BS/TV (mm^{-1})	4.14 ± 0.54	2.74 ± 0.18	0.049*
Tb.N (mm^{-3})	1.15 ± 0.15	0.70 ± 0.06	0.032*
Tb.Th (mm)	0.19 ± 0.03	0.16 ± 0.01	0.424
Tb.Sp (mm)	0.67 ± 0.08	0.81 ± 0.06	0.226
Conn.D.(mm^{-3})	9.40 ± 4.52	5.30 ± 1.77	0.430
SMI	1.19 ± 0.08	1.81 ± 0.12	0.005*

*$p < 0.05$

Enrichment of GO analysis

GO annotation was made to categorize 219 differentially expressed proteins based on 3 biological function types termed, molecular function (MF), cellular component (CC), and biological process (BP). To detect significantly enriched biological function types, we performed GO enrichment analysis and ranked terms by enrichment score (− log10(p value)). According to the GO enrichment results, for the upregulated proteins, there were 50 GO terms of MF, 59 GO terms of CC, and 322 GO terms of BP. For the downregulated proteins, there were 19, 41, and 151 GO terms of MF, CC, and BP, respectively. The top 8 significantly enriched MF terms, 8 significantly enriched CC terms, and 14 significantly enriched BP terms are shown in Fig. 1. The upregulated proteins were significantly enriched in MF terms related to proteasome function and transcription such as proteasome-activating ATPase activity ($p = 3.79 \times 10^{-7}$) and transcription factor activity, transcription factor binding ($p = 0.000217$). The most enriched CC terms, such as proteasome regulatory particle ($p = 1.39 \times 10^{-9}$), mainly associated with the proteasome. These proteins were also enriched in a wide range of biological processes, such as cellular macromolecule catabolic process ($p = 7.04 \times 10^{-10}$), RNA processing ($p = 3.23 \times 10^{-9}$), and non-canonical Wnt signaling pathway ($p = 1.82 \times 10^{-7}$). For down-regulated proteins, the most enriched MF terms included antigen binding ($p = 6.38 \times 10^{-10}$) and immunoglobulin receptor binding ($p = 1.02 \times 10^{-5}$), which were related to immune function. As for CC terms, they were enriched in immunoglobulin complex, circulating ($p = 6.83 \times 10^{-7}$), plasma membrane ($p = 5.25 \times 10^{-5}$), and podosome ($p = 0.000528$). Moreover, they were involved in phagocytosis ($p = 1.65 \times 10^{-9}$), adaptive immune response ($p = 3.21 \times 10^{-8}$), and cell migration ($p = 4.12 \times 10^{-7}$) biological processes. These results suggested that upregulated proteins were mainly associated with the regulation of transcription and protein metabolism, and downregulated proteins were involved in immune response and movements of the cell and cellular components.

Enrichment of KEGG pathway analysis

There was a total of 37 pathways generated from KEGG based on all differentially expressed proteins. And we set $p < 0.05$ as a cutoff for further enrichment analysis. These differentially

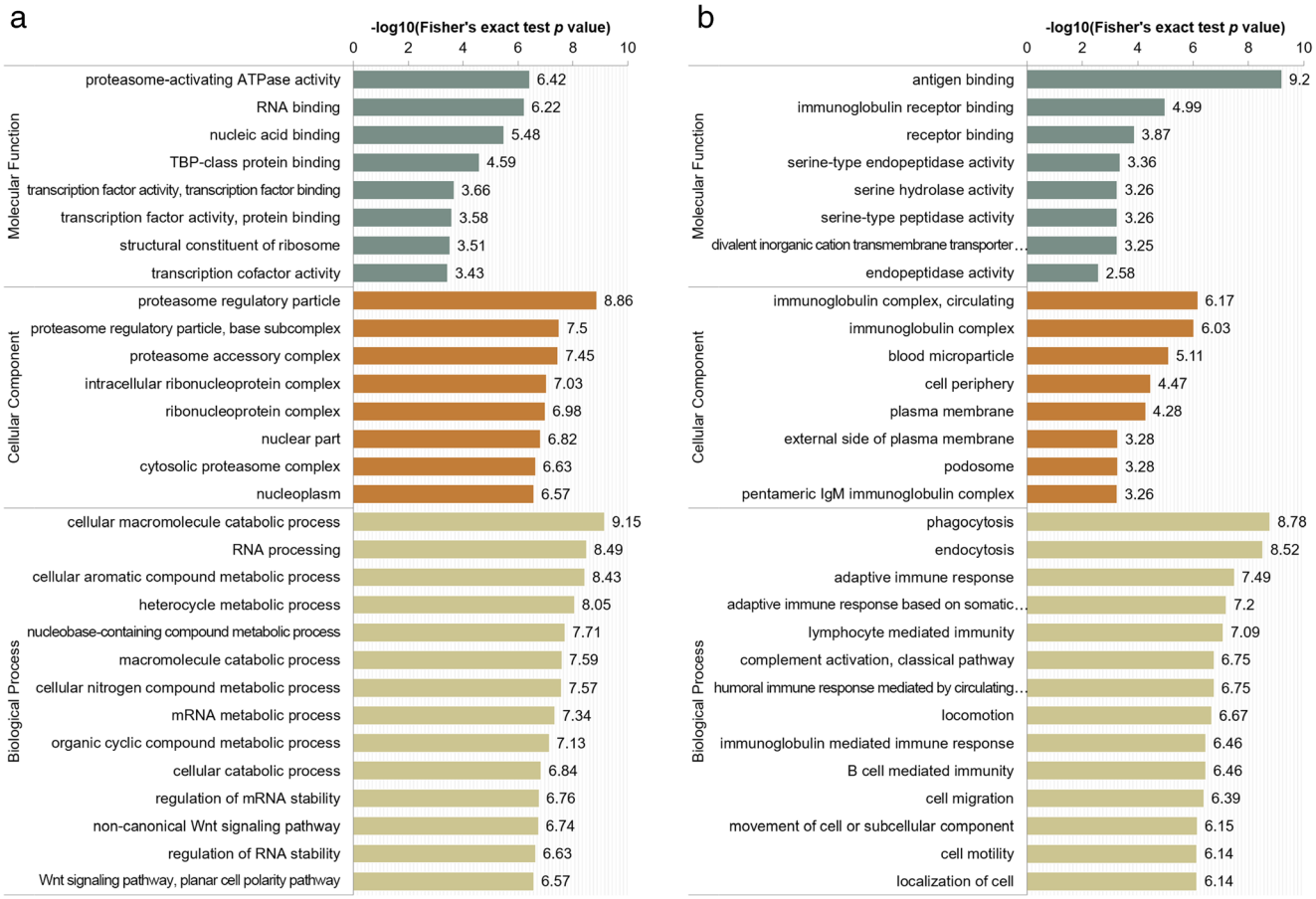

Fig. 1 Enrichment of GO analysis. The top 8 significantly enriched molecular function (MF) terms, 8 significantly enriched cellular component (CC) terms and 14 significantly enriched biological process (BP) terms are presented. The y-axis denotes the categories of GO terms. The x-axis denotes the enrichment score (−log10(*p* value)). **a** GO enrichment results of upregulated proteins. **b** GO enrichment results of downregulated proteins $p < 0.05$

expressed proteins were enriched in hsa03050 proteasome ($p = 0.000114$), followed by hsa03010 ribosome ($p = 0.002175$), hsa03320 PPAR signaling pathway ($p = 0.014193$), and some other pathways. The related proteins of hsa03050 proteasome included PSMC2, PSMC4, and PSMD14. RPL7A, RPL35A, and some other proteins were involved in hsa03010 ribosome. Besides, FABP4, PLIN1, PLIN4, CD36, ILK, and SORBS1 were associated with hsa03320 PPAR signaling pathway (Table 3).

PPI network of differentially expressed proteins

STRING is a database for assessing physical and functional protein–protein interactions. To understand the associations among these differentially expressed proteins, we constructed a PPI network by using the STRING database and applied Cytoscape software to visualize the network based on the regulation type, *p* value, fold change, interactions of proteins, and network clustering. Based on STRING predictions, we found that these differentially expressed proteins had multiple interactions. Interestingly, there were four closely co-expressed clusters of which proteins had high combined prediction scores with each other (Fig. 2). These clusters were mainly associated with spliceosome, ribosome, proteasome, and cytoskeleton. The spliceosome-related cluster included DDX5, YBX1, RAN, HNRNPM, and SNRPD2, which was involved in RNA splicing and transport. Proteins in the ribosome-related cluster included RPL35A, RPS2, RPS17, and XPO1. The proteasome-related cluster was comprised of PSMC2, PSMC6, VCP, etc. Proteins in the cytoskeleton-related cluster included PDLIM7, FERMT3, TLN1, and TPM4, and most of these proteins were downregulated.

Validation of DDX5, PSMC2, CSNK1A1, PLIN1, ILK, and TPM4

In consideration of the predicted functions, involved biological processes, fold changes, and protein–protein associations of these differentially expressed proteins, we selected DDX5, PSMC2, CSNK1A1, PLIN1, ILK, and TPM4 for further validation based on GO, KEGG, and PPI analysis results. Among these proteins, DDX5 (1.423-fold upregulated) was involved

Table 3 Enriched pathways and related proteins

KEGG pathway	Related proteins
hsa03050 Proteasome	PSMD2, PSMC2, PSMC6, PSMC5, PSMC1, PSMC4, PSMD4, PSMD14, PSMF1, PSMC3
hsa03010 Ribosome	RPL7A, RPL26, RPL35A, RPS2, RPS17, RPS15, RPL31, RPS19, RPS25, RPL17, RPS7, RPS24, RPS16, RPS8, RPS18, RPS4X, RPS23
hsa05320 Autoimmune thyroid disease	IGHV3-49, IGHV2-26, IGHV3-9, HLA-A
hsa05330 Allograft rejection	IGHV3-49, IGHV2-26, IGHV3-9, HLA-A
hsa03320 PPAR signaling pathway	FABP4, PLIN1, PLIN4, CD36, ILK, SORBS1
hsa04640 Hematopoietic cell lineage	IGHV3-49, IGHV2-26, CD36, IGHV3-9
hsa04961 Endocrine and other factor-regulated calcium reabsorption	AP2B1, DNM3, AP2M1, AP2A2, CLTB
hsa04721 Synaptic vesicle cycle	AP2B1, DNM3, AP2M1, AP2A2, NSF, CLTB
hsa03040 Spliceosome	PHF5A, TCERG1, SNRPD2, DDX5, SF3B2, SNRPC, SF3B5, SNRPN, HNRNPM, PRPF4, PRPF6

in regulation of osteoblast differentiation (GO:0045667), hsa03040 Spliceosome pathway, and had high combined scores with several differentially expressed proteins. PSMC2 (1.413-fold upregulated) took part in the osteoblast differentiation (GO:0001649), ubiquitin-dependent protein catabolic process (GO:0006511) and had multiple interactions with other proteins. For example, PSMC2 may have co-expression with XPO1 and YBX1, and binding action with VCP. CSNK1A1 (1.555-fold upregulated) were thought to participate in β-catenin destruction complex assembly (GO:1904885) and hsa04310 Wnt signaling pathway. PLIN1 (1.902-fold upregulated) had lipid binding (GO:0008289) function, participated in lipid metabolic process (GO:0006629), and was involved in hsa03320 PPAR

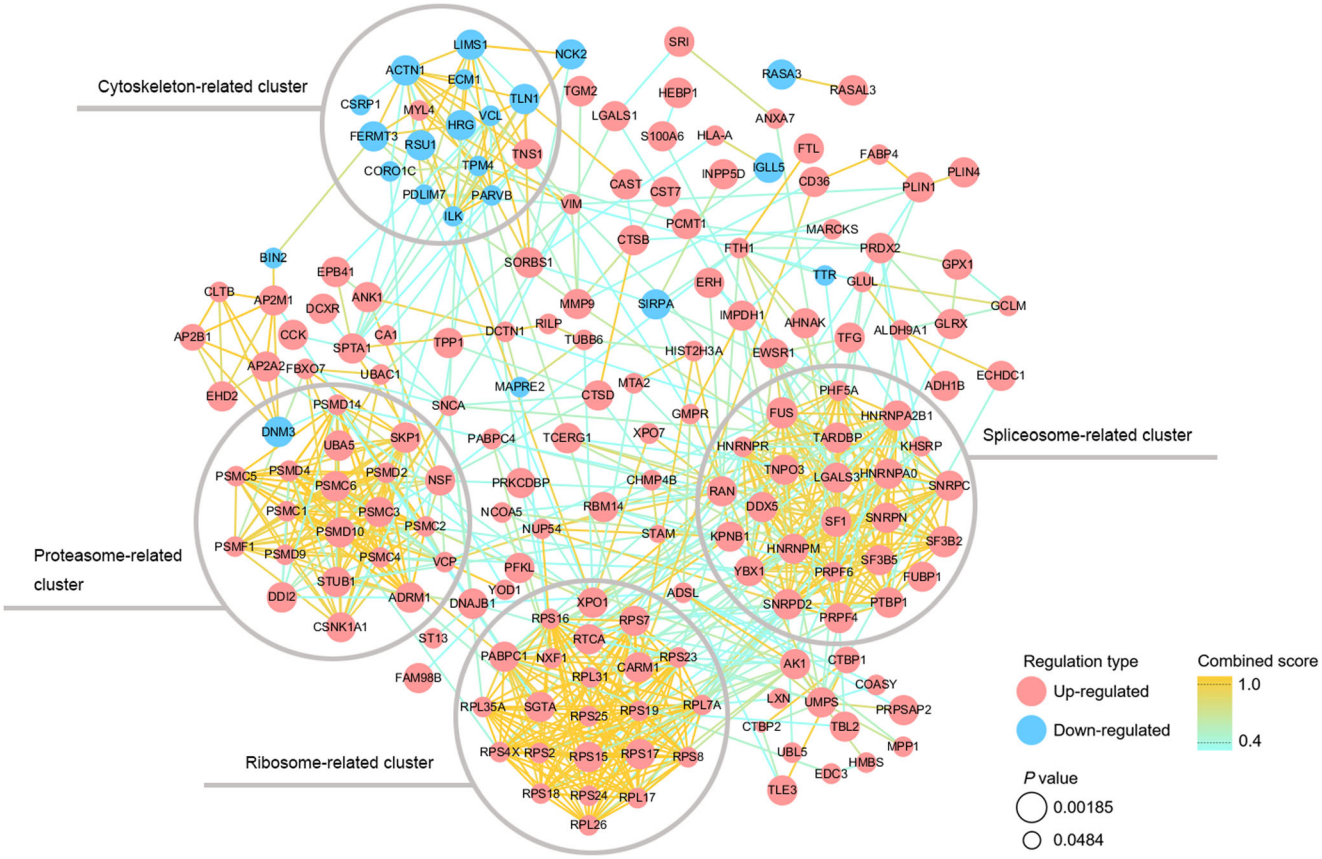

Fig. 2 Protein–protein network. Node color represents the regulation type. Node size represents *p* value. Line color represents the combined score (the reliability of protein–protein interaction). The closer the score is to 1, the more reliable the interaction is

signaling pathway. As for downregulated proteins, ILK (0.745-fold downregulated) was associated with positive regulation of BMP signaling pathway (GO:0030513) and positive regulation of canonical Wnt signaling pathway (GO:0090263). TPM4 (0.502-fold downregulated) was involved in the actin filament organization (GO:0007015). We further performed western blotting to explore the expressions of DDX5, PSMC2, CSNK1A1, PLIN1, ILK, and TPM4 in the validation group (Fig. 3a). The relative expressions of DDX5, PSMC2, and PLIN1 in OP were significantly higher than in non-OP ($p < 0.01$), and the relative expressions of ILK and TPM4 were significantly decreased in OP ($p < 0.01$) (Fig. 3b), which correspond with the high-throughput proteomics data. The relative expression of CSNK1A1/GAPDH showed no significant difference (Fig. 3b).

Discussion

The understanding of the connection between protein changes in the bone marrow and regulation of bone formation/resorption is relatively scarce, and the assessment of the holistic protein expression under pathological condition is mainly limited to serum or blood cells. Thus, we used a TMT-based high-throughput proteomics strategy to directly screen differentially abundant proteins in the bone marrow microenvironment. In this study, strict exclusion criteria were set for the study subjects, and the bone microstructural features of osteoporotic patients were significantly deteriorated. The overlap of quantified proteins was high among different samples as 1718 proteins could be quantitatively analyzed in each single sample. Using the 1.3-fold change cutoff, we found that 172 proteins in the BMSF of OP were increased compared with non-OP, and 47 were decreased. Bioinformatics tools were performed to analyze these proteins. Moreover, we verified some crucial proteins in the validation group.

Changes of proteins in this study suggest that these differentially expressed proteins may play essential roles in the pathogenesis of osteoporosis. The network-based analysis provided an integrative insight of differentially expressed proteins, since proteins in each cluster may function together or co-express in the pathogenesis of osteoporosis. Through PPI analysis, we identified four regulatory mechanisms, namely splicing, translation, protein degradation, and cytoskeletal organization corresponding to spliceosome, ribosome, proteasome, and cytoskeleton-related clusters. Strikingly, spliceosome, ribosome, and proteasome-related clusters were closely associated with post-transcriptional, translational, and post-translational level regulation. Specifically, alterations of spliceosome components and regulators can affect mRNA processing and maturation, which is growing recognized as the cause of numerous human disorders [20]. The ribosome is the initial site for protein biosynthesis and the hub of protein

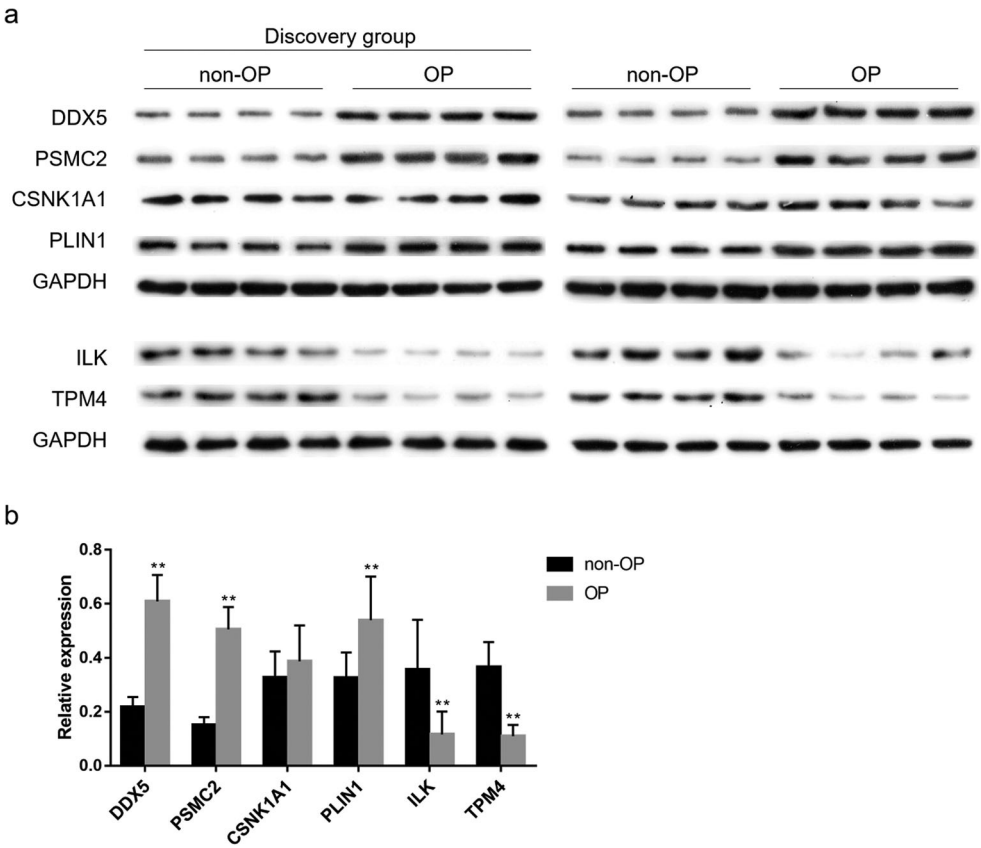

Fig. 3 Western blotting validation **a** western blotting results of up- and downregulated proteins. **b** Western blotting quantitative analysis. Internal control was GAPDH. $^{**}p < 0.01$, $n = 8$

quality control. Ubiquitin–proteasome system is one of the main mechanisms of protein quality control since it acts a pivotal part in maintaining protein homeostasis by proteasome-mediated degradation of ubiquitinated proteins. Besides, the cytoskeletal organization is involved in cell proliferation, adhesion, and migration. Aberrant cytoskeletal structures may affect the function of osteoclasts and osteoblasts [21–23]. Moreover, these four clusters do not work independently but have complex interactions. mRNA processing is associated with the translation mechanism; meanwhile, the proteasome system degrades abnormal proteins produced by the translation of defective mRNA and mistakes in protein synthesis [24]. And ubiquitylation of cytoskeletal components controls cell adhesion and migration [25]. Correspondingly, based on our results, proteins from different clusters have multiple associations. For instance, XPO1 (exportin-1) was an upregulated protein in the ribosome-related cluster, and ILK (integrin-linked protein kinase) was a downregulated protein in the cytoskeleton-related cluster in our study. Inhibition of XPO1 increases nuclear expression ILK and reduces osteoclast differentiation, which is involved in osteolytic bone lesions of some cancers [26]. Consequently, these differentially expressed clusters support the idea that the pathogenesis of osteoporosis involves changes in several tightly connected key phases of gene regulatory mechanisms and proteostasis. The interactions of these proteins may provide some new ideas for in-depth mechanism studies, helping to discover novel therapeutic targets for osteoporosis.

We further verified some proteins in these major clusters. Our results showed that DDX5 (DEAD box protein 5) was a crucial protein in the spliceosome-related cluster. DDX5 is a regulator of gene expression. It is essential for adipogenic differentiation at the early stage [27] and inhibits osteogenic differentiation of mesenchymal progenitors [28]. However, when cells are committed to osteoblast lineage, DDX5 functions as the transcriptional co-activator of RUNX2 [28]. According to our TMT-based proteomics results and western blotting results, DDX5 was upregulated in OP. Nonetheless, many questions about the role that DDX5 plays in osteogenesis or adipogenesis remain to be answered.

Additionally, we verified PSMC2 (26S protease regulatory subunit 7), an upregulated protein in the proteasome-related cluster. Proteasome-mediated ubiquitin-dependent degradation is involved in the regulation of RUNX2 [29] and ubiquitinated phospho-β-catenin [30]. It is worth noting that CSNK1A1 (casein kinase I isoform α), another upregulated protein in the proteasome-related cluster, is a component of β-catenin destruction complex which regulates canonical Wnt signaling. Briefly, β-catenin is phosphorylated by this destruction complex, then ubiquitinated by the SCF-β-TrCP1. Subsequently, ubiquitinated phospho-β-catenin is degraded by the 26S proteasome [31]. These indicate that PSMC2 has a negative regulation on Wnt signaling pathway and CSNK1A1 has a positive regulation of proteasomal degradation of ubiquitinated proteins involved in osteoblast differentiation. However, western blotting results revealed no significant difference of CSNK1A1 abundance between OP and non-OP. This may be due to individual diversity or false positive of proteomics analysis, and a larger sample volume validation may be needed.

Based on the network analysis, a majority of proteins in the cytoskeleton-related cluster was downregulated, such as ILK and TPM4. ILK (integrin-linked kinase) is a mediator in the integrin-actin cytoskeleton connection and integrin-mediated signal transduction [32]. The roles of integrins in bone homeostasis have been widely discussed. A previous study found that integrins in serum-derived exosomes were downregulated in osteoporotic patients and serum-derived exosomes of osteoporotic patients inhibited osteoblast formation and promoted osteoclast differentiation in vitro [14]. However, the role of ILK in skeletal biology has not been fully understood. Interestingly, some studies found that loss of ILK in osteoblast lineage led to impaired osteoblast function and decreased bone mineralization [21], whereas osteoclast-specific Ilk ablation mice exhibited reduced resorptive capacity and increased bone volume [33]. Also, TPM4 (tropomyosin α4) is a member of tropomyosins, a family of actin-binding proteins that are essential for cellular morphogenesis, motility, and adhesiveness [34]. It has been suggested that TPM4 stabilizes attachment structures of osteoclasts, including podosomes and sealing zone [35, 36]. Thus, these cytoskeleton-associated proteins may affect the cellular migration and adhesion of osteoblasts and osteoclasts, thereby exerting an integrative influence on both bone formation and bone resorption.

In addition to the four clusters mentioned above, lipid metabolism-related proteins did not form a distinct cluster, but they are also noteworthy. It is suggested that marrow adiposity is linked with reduced bone quantity and quality [37]. PLIN1 (perilipin-1) is a modulator of adipocyte lipid metabolism. Under basal states, it protects triglyceride stored in lipid droplets from lipolysis; while under β-adrenergic stimulation, it facilitates lipolysis [38]. Overexpression of PLIN1 increases total triglyceride accumulation and enlarges lipid droplet in adipocytes [39]. Triglyceride is the main lipid content of adipose tissue in bone marrow microenvironment [37]. When needed, triglyceride releases free fatty acids which can modulate osteoblastogenesis [8]. We speculate that PLIN1 may affect bone homeostasis by regulating triglyceride storage and fatty acid levels. And the exact mechanism of PLIN1 in osteogenesis and adipogenesis requires more researches to confirm.

We emphasize that the current study is a preliminary exploration of the proteins in bone marrow microenvironment. We will focus on some potential target proteins in the future for in-depth research on the underlying mechanisms of osteoporosis. Furthermore, since the bone microstructure and bone marrow microenvironment of osteoporotic patients undergoing spine fusion have changed, it is recommended that surgeons perform routine osteoporosis-related checkups such as

the BMD examination and proper preoperative assessments. For patients with osteoporosis, surgical procedures should be adjusted to avoid fusion construct failure, such as using instrumentation at multiple levels [40].

Conclusion

TMT-based proteomics technology provides a new method for the identification of proteins in the bone marrow microenvironment. Multiple protein factors, such as DDX5, PSMC2, CSNK1A1, PLIN1, ILK, and TPM4, differentially expressed in the bone marrow microenvironment of osteoporotic patients. Splicing, translation, protein degradation, cytoskeletal organization, and lipid metabolism may be the key regulatory mechanisms involved in the pathogenesis of osteoporosis.

Acknowledgments We thank Shanghai Jiao Tong University Affiliated Sixth People's Hospital (Shanghai, China) for providing us with SkyScan1176 to perform micro-CT and Jingjie PTM BioLab (Hangzhou, China) for the technical support.

Funding Information This research is supported by the National Natural Science Foundation of China (81670804), the Science and Technology Program of Hunan Province (2016WK2020) and the Clinical Big Data Project of Central South University.

Compliance with ethical standards

This study obtained the ethics approval from the ethical committee of the Second Xiangya Hospital.

Conflicts of interest None.

References

1. Rachner TD, Khosla S, Hofbauer LC (2011) Osteoporosis: now and the future. Lancet 377(9773):1276–1287. https://doi.org/10.1016/S0140-6736(10)62349-5
2. Collin-Osdoby P (1994) Role of vascular endothelial cells in bone biology. J Cell Biochem 55(3):304–309. https://doi.org/10.1002/jcb.240550306
3. Li J, Liu X, Zuo B, Zhang L (2016) The role of bone marrow microenvironment in governing the balance between osteoblastogenesis and adipogenesis. Aging Dis 7(4):514–525. https://doi.org/10.14336/AD.2015.1206
4. Feng X, McDonald JM (2011) Disorders of bone remodeling. Annu Rev Pathol 6:121–145. https://doi.org/10.1146/annurev-pathol-011110-130203
5. Moore KA, Lemischka IR (2006) Stem cells and their niches. Science 311(5769):1880–1885. https://doi.org/10.1126/science.1110542
6. Bai XC, Lu D, Bai J, Zheng H, Ke ZY, Li XM, Luo SQ (2004) Oxidative stress inhibits osteoblastic differentiation of bone cells by ERK and NF-kappaB. Biochem Biophys Res Commun 314(1):197–207
7. Gillet C, Dalla Valle A, Gaspard N, Spruyt D, Vertongen P, Lechanteur J, Rigutto S, Dragan ER, Heuschling A, Gangji V, Rasschaert J (2017) Osteonecrosis of the femoral head: lipotoxicity exacerbation in MSC and modifications of the bone marrow fluid. Endocrinology 158(3):490–502. https://doi.org/10.1210/en.2016-1687
8. Elbaz A, Wu X, Rivas D, Gimble JM, Duque G (2010) Inhibition of fatty acid biosynthesis prevents adipocyte lipotoxicity on human osteoblasts in vitro. J Cell Mol Med 14(4):982–991. https://doi.org/10.1111/j.1582-4934.2009.00751.x
9. Xie F, Zhou B, Wang J, Liu T, Wu X, Fang R, Kang Y, Dai R (2018) Microstructural properties of trabecular bone autografts: comparison of men and women with and without osteoporosis. Arch Osteoporos 13(1):18. https://doi.org/10.1007/s11657-018-0422-z
10. Zeng Y, Zhang L, Zhu W, He H, Sheng H, Tian Q, Deng FY, Zhang LS, Hu HG, Deng HW (2017) Network based subcellular proteomics in monocyte membrane revealed novel candidate genes involved in osteoporosis. Osteoporos Int 28(10):3033–3042. https://doi.org/10.1007/s00198-017-4146-5
11. Nielson CM, Wiedrick J, Shen J, Jacobs J, Baker ES, Baraff A, Piehowski P, Lee CG, Baratt A, Petyuk V, McWeeney S, Lim JY, Bauer DC, Lane NE, Cawthon PM, Smith RD, Lapidus J, Orwoll ES, Osteoporotic Fractures in Men Study Research G (2017) Identification of hip BMD loss and fracture risk markers through population-based serum proteomics. J Bone Miner Res 32(7):1559–1567. https://doi.org/10.1002/jbmr.3125
12. Zhu W, Shen H, Zhang JG, Zhang L, Zeng Y, Huang HL, Zhao YC, He H, Zhou Y, Wu KH, Tian Q, Zhao LJ, Deng FY, Deng HW (2017) Cytosolic proteome profiling of monocytes for male osteoporosis. Osteoporos Int 28(3):1035–1046. https://doi.org/10.1007/s00198-016-3825-y
13. Zhang L, Liu YZ, Zeng Y, Zhu W, Zhao YC, Zhang JG, Zhu JQ, He H, Shen H, Tian Q, Deng FY, Papasian CJ, Deng HW (2016) Network-based proteomic analysis for postmenopausal osteoporosis in Caucasian females. Proteomics 16(1):12–28. https://doi.org/10.1002/pmic.201500005
14. Xie Y, Gao Y, Zhang L, Chen Y, Ge W, Tang P (2018) Involvement of serum-derived exosomes of elderly patients with bone loss in failure of bone remodeling via alteration of exosomal bone-related proteins. Aging Cell 17(3):e12758. https://doi.org/10.1111/acel.12758
15. Miranda M, Pino AM, Fuenzalida K, Rosen CJ, Seitz G, Rodriguez JP (2016) Characterization of fatty acid composition in bone marrow fluid from postmenopausal women: modification after hip fracture. J Cell Biochem 117(10):2370–2376. https://doi.org/10.1002/jcb.25534
16. Pino AM, Rios S, Astudillo P, Fernandez M, Figueroa P, Seitz G, Rodriguez JP (2010) Concentration of adipogenic and proinflammatory cytokines in the bone marrow supernatant fluid of osteoporotic women. J Bone Miner Res 25(3):492–498. https://doi.org/10.1359/jbmr.090802
17. Wiig H, Berggreen E, Borge BA, Iversen PO (2004) Demonstration of altered signaling responses in bone marrow extracellular fluid during increased hematopoiesis in rats using a centrifugation method. Am J Physiol Heart Circ Physiol 286(5):H2028–H2034. https://doi.org/10.1152/ajpheart.00934.2003
18. Moulder R, Bhosale SD, Goodlett DR, Lahesmaa R (2017) Analysis of the plasma proteome using iTRAQ and TMT-based isobaric labeling. Mass Spectrom Rev 37:583–606. https://doi.org/10.1002/mas.21550
19. Thompson A, Schafer J, Kuhn K, Kienle S, Schwarz J, Schmidt G, Neumann T, Johnstone R, Mohammed AK, Hamon C (2003) Tandem mass tags: a novel quantification strategy for comparative

analysis of complex protein mixtures by MS/MS. Anal Chem 75(8):1895–1904
20. Chabot B, Shkreta L (2016) Defective control of pre-messenger RNA splicing in human disease. J Cell Biol 212(1):13–27. https://doi.org/10.1083/jcb.201510032
21. Dejaeger M, Bohm AM, Dirckx N, Devriese J, Nefyodova E, Cardoen R, St-Arnaud R, Tournoy J, Luyten FP, Maes C (2017) Integrin-linked kinase regulates bone formation by controlling cytoskeletal organization and modulating BMP and Wnt signaling in Osteoprogenitors. J Bone Miner Res 32(10):2087–2102. https://doi.org/10.1002/jbmr.3190
22. Higuchi C, Nakamura N, Yoshikawa H, Itoh K (2009) Transient dynamic actin cytoskeletal change stimulates the osteoblastic differentiation. J Bone Miner Metab 27(2):158–167. https://doi.org/10.1007/s00774-009-0037-y
23. Novack DV, Faccio R (2011) Osteoclast motility: putting the brakes on bone resorption. Ageing Res Rev 10(1):54–61. https://doi.org/10.1016/j.arr.2009.09.005
24. Wang F, Canadeo LA, Huibregtse JM (2015) Ubiquitination of newly synthesized proteins at the ribosome. Biochimie 114:127–133. https://doi.org/10.1016/j.biochi.2015.02.006
25. Schaefer A, Nethe M, Hordijk PL (2012) Ubiquitin links to cytoskeletal dynamics, cell adhesion and migration. Biochem J 442(1):13–25. https://doi.org/10.1042/BJ20111815
26. Gravina GL, Tortoreto M, Mancini A, Addis A, Di Cesare E, Lenzi A, Landesman Y, McCauley D, Kauffman M, Shacham S, Zaffaroni N, Festuccia C (2014) XPO1/CRM1-selective inhibitors of nuclear export (SINE) reduce tumor spreading and improve overall survival in preclinical models of prostate cancer (PCa). J Hematol Oncol 7:46. https://doi.org/10.1186/1756-8722-7-46
27. Ramanathan N, Lim N, Stewart CL (2015) DDX5/p68 RNA helicase expression is essential for initiating adipogenesis. Lipids Health Dis 14:160. https://doi.org/10.1186/s12944-015-0163-6
28. Jensen ED, Niu L, Caretti G, Nicol SM, Teplyuk N, Stein GS, Sartorelli V, van Wijnen AJ, Fuller-Pace FV, Westendorf JJ (2008) p68 (Ddx5) interacts with Runx2 and regulates osteoblast differentiation. J Cell Biochem 103(5):1438–1451. https://doi.org/10.1002/jcb.21526
29. Kumar Y, Kapoor I, Khan K, Thacker G, Khan MP, Shukla N, Kanaujiya JK, Sanyal S, Chattopadhyay N, Trivedi AK (2015) E3 ubiquitin ligase Fbw7 negatively regulates osteoblast differentiation by targeting Runx2 for degradation. J Biol Chem 290(52):30975–30987. https://doi.org/10.1074/jbc.M115.669531
30. Calviello G, Resci F, Serini S, Piccioni E, Toesca A, Boninsegna A, Monego G, Ranelletti FO, Palozza P (2007) Docosahexaenoic acid induces proteasome-dependent degradation of beta-catenin, down-regulation of survivin and apoptosis in human colorectal cancer cells not expressing COX-2. Carcinogenesis 28(6):1202–1209. https://doi.org/10.1093/carcin/bgl254
31. Kimelman D, Xu W (2006) Beta-catenin destruction complex: insights and questions from a structural perspective. Oncogene 25(57):7482–7491. https://doi.org/10.1038/sj.onc.1210055
32. Brakebusch C, Fassler R (2003) The integrin-actin connection an eternal love affair. EMBO J 22(10):2324–2333. https://doi.org/10.1093/emboj/cdg245
33. Dossa T, Arabian A, Windle JJ, Dedhar S, Teitelbaum SL, Ross FP, Roodman GD, St-Arnaud R (2010) Osteoclast-specific inactivation of the integrin-linked kinase (ILK) inhibits bone resorption. J Cell Biochem 110(4):960–967. https://doi.org/10.1002/jcb.22609
34. Gimona M, Kazzaz JA, Helfman DM (1996) Forced expression of tropomyosin 2 or 3 in v-Ki-ras-transformed fibroblasts results in distinct phenotypic effects. Proc Natl Acad Sci U S A 93(18):9618–9623
35. McMichael BK, Kotadiya P, Singh T, Holliday LS, Lee BS (2006) Tropomyosin isoforms localize to distinct microfilament populations in osteoclasts. Bone 39(4):694–705. https://doi.org/10.1016/j.bone.2006.04.031
36. McMichael BK, Lee BS (2008) Tropomyosin 4 regulates adhesion structures and resorptive capacity in osteoclasts. Exp Cell Res 314(3):564–573. https://doi.org/10.1016/j.yexcr.2007.10.018
37. Fazeli PK, Horowitz MC, MacDougald OA, Scheller EL, Rodeheffer MS, Rosen CJ, Klibanski A (2013) Marrow fat and bone—new perspectives. J Clin Endocrinol Metab 98(3):935–945. https://doi.org/10.1210/jc.2012-3634
38. Brasaemle DL (2007) Thematic review series: adipocyte biology. The perilipin family of structural lipid droplet proteins: stabilization of lipid droplets and control of lipolysis. J Lipid Res 48(12):2547–2559. https://doi.org/10.1194/jlr.R700014-JLR200
39. Grahn TH, Zhang Y, Lee MJ, Sommer AG, Mostoslavsky G, Fried SK, Greenberg AS, Puri V (2013) FSP27 and PLIN1 interaction promotes the formation of large lipid droplets in human adipocytes. Biochem Biophys Res Commun 432(2):296–301. https://doi.org/10.1016/j.bbrc.2013.01.113
40. Lehman RA Jr, Kang DG, Wagner SC (2015) Management of osteoporosis in spine surgery. J Am Acad Orthop Surg 23(4):253–263. https://doi.org/10.5435/JAAOS-D-14-00042